

# Ultrastable frequency reference at 1.56 $\mu$ m using a $^{12}\text{C}^{16}\text{O}$ molecular overtone transition with the noise-immune cavity-enhanced optical heterodyne molecular spectroscopy method

SHAILENDHAR SARAF<sup>\*</sup>, PAUL BERCEAU, ALBERTO STOCHINO, ROBERT BYER, AND JOHN LIPA

Hansen Experimental Physics Laboratory, Stanford University, Stanford, CA 94305 USA

\*Corresponding author: [saraf@stanford.edu](mailto:saraf@stanford.edu)

Received XX Month XXXX; revised XX Month, XXXX; accepted XX Month XXXX; posted XX Month XXXX (Doc. ID XXXXX); published XX Month XXXX

**We report on an ultrastable molecular clock based on the interrogation of the 3v rotational-vibrational combination band at 1563nm of carbon monoxide  $^{12}\text{C}^{16}\text{O}$ . The laser stabilization scheme is based on frequency modulation (FM) saturation spectroscopy in a high-finesse ultra-low expansion (ULE) glass optical cavity using CO as the molecular reference for long-term stabilization of the cavity resonance. The NICE-OHMS FM modulation method is employed to maintain a high signal-to-noise ratio and avoid conversion of laser frequency noise into amplitude noise by the high finesse cavity. We report an Allan Deviation of  $1.8 \times 10^{-12}$  at 1 second that improves to  $3.5 \times 10^{-14}$  after 1000 seconds of averaging. © 2015 Optical Society of America**

**OCIS codes:** (300.6340) Spectroscopy, infrared; (300.6360) Spectroscopy, laser; (300.6380) Spectroscopy, modulation; (120.3940) Metrology.

<http://dx.doi.org/10.1364/OL.99.099999>

There are several applications for compact ultrastable frequency standards for use in space. Advanced GNSS systems, tests of fundamental physics, formation flying, and gravitational wave detectors [1] are some of the applications that require high fidelity frequency standards. The STAR experiment [2] is another example of the need for a space-based ultrastable clock for rod-clock type experiments designed to test Lorentz invariance. Molecular clocks based on modulation transfer spectroscopy (MTS) using an electronic transition of  $^{127}\text{I}_2$  interrogated at 532nm have been developed for space applications [3]. However, these clocks need precise pointing control, have magnetic sensitivity and are limited to  $10^{-14}$  frequency stability at short timescales [4]. Our objective is to advance the development of a laser stabilization scheme that has very low noise into a unit that is low power and compact,

and can be used in space for missions requiring extreme performance in optical frequency stabilization. Insensitivity to DC and AC magnetic fields is required for these clocks, especially payloads operating in a Low Earth Orbit. It is also desirable to operate the laser system at telecom wavelengths to take advantage of the significant infrastructure for optical components like fibers, modulators, compact and single-frequency diode lasers. Our device operates near 1563 nm using low pressure CO gas as a molecular reference and a spectroscopic technique that has been demonstrated using gases such as  $\text{C}_2\text{HD}$ ,  $\text{C}_2\text{H}_2$  and  $\text{CO}_2$  [5-7]. Its ultimate performance as a stabilization system using CO, based on calculation [8], is expected to approach that of ultra-cold neutral atom clocks that require multiple lasers and an extensive amount of equipment. The lighter and simpler package that we are developing will allow the realization of a more practical ultrastable reference for space use.

Molecular overtones provide many rotation-vibrational comb-like resonances that cover a broad spectrum in the visible and near-IR regions, while the linewidths potentially are in the sub-kilohertz domain that is characteristic of the decay rates of fundamental molecular stretch resonances. For frequency stabilization purposes, we need to observe saturated absorption resonances to achieve the necessary narrow sub-Doppler linewidths that are inevitably broadened well beyond the decay rate. The weak absorption of these overtone transitions requires high optical powers to achieve saturation. For example, a typical cavity power needed for  $\text{C}_2\text{HD}$  ( $\nu_2+3\nu_3$ ) $P(5)$  transition is  $>100$  W at  $\sim 1$  mTorr for the 1064nm transitions [5]. For the 1560 nm CO transitions, the cavity power needed for saturation is  $\sim 2$ W at 10 mTorr. Thus for these transitions we are led to consider cavities of high finesse to yield large power buildup inside the cavity, giving good saturation parameters without requiring a large transmitted power to be accepted by the detector. However, the cavity with high finesse naturally becomes an efficient laser-frequency

discriminator, leading to conversion of residual laser-frequency noise into amplitude noise [6].

In conjunction with saturation spectroscopy, FM spectroscopy avoids excessive amplitude noise, by performing modulation and detection of the signal in a frequency region where noise processes of whatever origin no longer possess strong power density. The NICE-OHMS technique [5-7,9,10] captures the advantages of both FM detection and intracavity absorption enhancement while eliminating sensitivity to the laser/cavity relative frequency noise. The frequency offset of the modulation sidebands for FM detection is actively controlled to fall exactly on axial cavity resonances, shifted by one or more cavity free spectral range (FSR). Therefore, for small frequency shifts of the laser and its sidebands about the exact cavity modes, all experience the same small amplitude jitter and phase shifts for their internal fields. Thus the transmitted beam remains purely FM despite small power fluctuations on the detector, and no unwanted detected noise results from small laser-cavity detunings at the modulation frequency, thus rendering the spectroscopic method as being frequency-noise immune [6]. Thus the noise level can approach the intrinsic AM noise level of the laser at the  $\frac{c}{2L}$  FM detection frequency. Here  $c$  is the velocity of light and  $L$  is the cavity length.

Here we report, the first NICE-OHMS based molecular clock at telecom wavelength interrogating a narrow overtone transition of carbon monoxide. CO is an attractive molecule for metrology as it has several rotational-vibrational transitions and associated overtone bands that can be interrogated with commercially available near-IR lasers. The total rotational-vibrational energy calculation yields a spectrum for the diatomic CO molecule with the R and P branches on each side of the band origin [11]. In the case of CO, the strongest transition for the 2<sup>nd</sup> overtone ( $\Delta v = 3$ ) is the R(7) line at 1568.038nm. In the early stage of our experiment, the laser source customized to interrogate this transition was noisy causing us to change to the weaker R(14) line at 1563.618nm. Key spectroscopic parameters for CO [10] are  $\alpha_0$ , the small-signal absorption coefficient  $2.2 \times 10^{-8}$  cm<sup>-1</sup>/mTorr for the R(14) line at 1563.618 nm [8]. Pressure broadening coefficient is 5.11 kHz/ mTorr while the pressure shift is -213 Hz/ mTorr. The Doppler broadened linewidth at 25 C is 443 MHz (FWHM). Band origin for the 3v band is at 6429.9 cm<sup>-1</sup>. Dipole moment for this transition extracted from Hitran data [12,13] is 0.41 mDebye. The saturation power based on this calculated dipole moment at the operating gas pressure of 9.5 mTorr is a fairly reasonable and attainable 1.95 W. Frequency shifts from Zeeman splitting are <4 MHz/Tesla [14].

At the heart of the experiment is a 25.6 cm optical cavity formed by a ULE spacer between a flat and ROC = 50 cm supermirrors. The cavity is installed on a V-block inside an aluminum can (CO reacts with nickel) that can be filled with CO gas at a desired pressure, usually set at 9.5 mT. The fused-silica substrate matched supermirrors (Advanced Thin Films) are attached to PZTs (Piezomechanik, 150/14-10/12) that are mounted on the ULE spacer. The cavity FSR is 585 MHz, the spot sizes (radii) on the flat mirror and curved mirror are calculated at 353  $\mu$ m and 504  $\mu$ m, respectively. The average spot radius for the Gaussian TEM<sub>00</sub> beam in the cavity for estimating the transit-time broadening is calculated at 411  $\mu$ m. The cold-cavity finesse using a ring-down measurement is 170,000, yielding a round-trip cavity loss of 37 ppm. Mirror loss is estimated at 8 ppm, therefore the transmittance of the output mirror is calculated to be 10.5 ppm. Transit time broadening for a spot of diameter 822

$\mu$ m and the most probable speed of CO molecules at room temperature is calculated at 257 kHz. Operating at a pressure of 9.5 mTorr, the molecular linewidth becomes 308 kHz. Since we operate at the optimal saturation parameter  $s = 0.8$ , the power broadened linewidth is 413 kHz. The single-pass small-signal integrated absorption  $\alpha_0 L$  for the R(14) line at 9.5 mTorr is calculated to be 5.5 ppm. The absolute level  $\Delta \alpha L$  of saturated absorption by the CO molecules inside the cavity is given by the equation:

$$\Delta \alpha L = \left( \frac{\alpha_0 L}{\sqrt{1+s}} - \frac{\alpha_0 L}{\sqrt{1+2s}} \right). \quad (1)$$

Therefore the absolute level of saturated absorption in our CO cavity based on a measured peak contrast of 12.5% is 0.69 ppm. This number divided by the measured S/N from the NICE-OHMS detection system [7] will yield the noise-equivalent detection sensitivity of the spectrometer and is estimated below.

The non-resonant single-pass cavity gas absorption plus mirror loss for an optimal saturation parameter  $s = 0.8$  is 12.1 ppm. However, at line center with 2-beam saturation the single-pass absorption is 11.4 ppm. The resonant cavity Finesse based on these absorption numbers is calculated at 143,000 yielding a FWHM linewidth of 4.1 kHz. The cavity power buildup is 21,800. The input power for optimal saturation is about 90  $\mu$ W, assuming optimal coupling. Transmission coefficients off-resonance and on-resonance are 21.7% and 23%, respectively. The non-resonant and on-resonance transmitted powers are 19.4  $\mu$ W and 20.6  $\mu$ W, respectively. Therefore, the signal power is 1.2  $\mu$ W and assuming a photodetector efficiency of 0.95mA/mW, we obtain a S/N of  $4.7 \times 10^5$  at 1 second. The corresponding fractional frequency stability  $\delta \nu / \nu$ , is given by

$$\frac{\delta \nu}{\nu} \Big|_{1s} = \frac{\Delta \nu}{\nu} \frac{1}{S/N}, \quad (2)$$

where  $\nu$  is the laser frequency and  $\Delta \nu$  is the molecular transition linewidth. The molecular linewidth divided by the S/N is 0.87 Hz yielding a fractional frequency stability of  $4.5 \times 10^{-15}$  at 1 second. This will be the ultimate performance of the frequency standard. On the other hand, from a detection sensitivity perspective, the shot-noise-limited sensitivity [6] of the NICE-OHMS based CO spectrometer is given by

$$(\alpha L)_{\min} = \frac{\pi}{F} \sqrt{\frac{h \nu B}{\eta P_0}} \frac{1}{J_0(\beta) J_1(\beta)}, \quad (3)$$

where  $F$  is the cavity finesse,  $h$  is Planck's constant,  $B$  is the detection bandwidth,  $\eta$  is the detector's quantum efficiency,  $\gamma$  is the carrier frequency,  $P_0$  is the light power on the detector and  $\beta$  is the modulation index. Our CO spectrometer operated at the optimal  $\beta = 1.1$  and  $\eta = 0.95$  mA/mW, detection BW of  $1/2\pi$  Hz and  $P_0 = 1$  mW will yield a shot-noise-limited species detection sensitivity of  $3 \times 10^{-13}$ .

Figure 1 shows our experimental setup. The light source is a 10 mW single-frequency, narrow-linewidth external-cavity diode laser [15] at a custom wavelength of 1563.62 nm from Redfern Integrated Optics (RIO). The laser is first locked to a low-finesse ( $\sim 6000$ ) ULE pre-stabilization cavity in vacuum using a free-space double pass acousto-optic modulator (AOM), as shown on the top of Fig. 1. This suppresses the high frequency noise of the laser while a piezoelectric (PZT) transducers on a cavity mirror and cavity

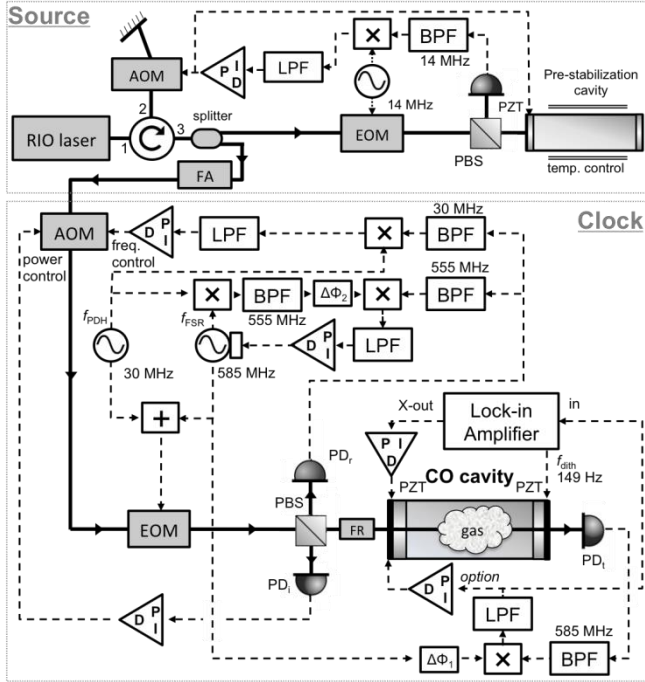


Fig. 1. Simplified layout of the experimental setup showing the light source and the NICE-OHMS stabilization system: AOM, acousto-optic modulator; EOM, electro-optic modulator; FA, fiber amplifier; PBS, polarizing beam splitter; FR, Faraday rotor; PID, servo control stages;  $f_{PDH}$ , PDH modulation frequency;  $f_{FSR}$ , free spectral range lock frequency;  $f_{dith}$ , dither frequency;  $PD_i$ , input power photodiode;  $PD_r$ , reflection photodiode;  $PD_t$ , transmission photodiode;  $\Delta\Phi_{1,2}$ , phase shifters; PZT, piezoelectric transducer; LPF, low-pass filter; BPF, band-pass filter; X, double balanced mixer.

temperature are the actuators for low frequency corrections. The power of the laser beam is then amplified to 150 mW by a fiber optical power amplifier (FA, PriTel, PMFA-30) to compensate for the relatively high insertion loss in the AOM and EOM. We then lock the laser to our ultra-high finesse Fabry-Perot cavity with the Pound-Drever-Hall (PDH) method [16]. To lock the laser on the cavity, a first pair of sidebands ( $f_{PDH} = 30$  MHz) with a modulation index  $\beta_1 \sim 0.4$  are added to the beam using an electro-optic modulator (EOM), and heterodyne detection of the beam reflected by the cavity is performed by the photodiode  $PD_r$  (Newfocus, 1611). This produces an error signal that is processed by a custom PID stage and then drives a fiber-coupled double-pass AOM (Brimrose, IPF-300-100-1550-2FP). Our servo bandwidth is 150 kHz and its gain is sufficient to provide a low frequency-noise density of  $0.05$  Hz/ $\sqrt{\text{Hz}}$  corresponding to a 51 mHz laser linewidth relative to the cavity [17]. The input power to the cavity is set at 1.1 mW and is stabilized using a small pickoff photodiode  $PD_i$  and a servo loop whose error signal drives the RF power sent to the AOM. The fractional power noise does not exceed  $10^{-3}$  typically. We then add a second pair of sidebands at  $f_{FSR} = 585$  MHz with a modulation index  $\beta_2 \sim 0.45$  using a signal generator (Stanford Research Systems, SG382) with an external modulation input and lock them to the FSR of the cavity by implementing the DeVoe-Brewer technique [18]. The heterodyne detection is performed by the photodiode  $PD_r$  at the frequency  $f_{FSR} - f_{PDH} = 555$  MHz, and the feedback signal is sent

to the external modulation port of the signal generator. The detection phase of the obtained error signal is optimized using the phase delay  $\Delta\Phi_2$  between the signal generator and the bandpass filtered signal from the reflection photodiode. The bandwidth of the FSR servo loop is about 10 kHz. The coupled carrier power into the cavity is estimated based on the modulation indices of the PDH and FSR sidebands and the reflected power. The coupling efficiency is about 12% and the circulating cavity power corresponds to a saturation parameter  $s \sim 0.8$ . Once the carrier and FSR-sidebands are resonant with the cavity we perform the heterodyne frequency detection in transmission with the photodiode  $PD_t$  (Newfocus, 1611) at  $f_{FSR}$ . The carrier is brought on the resonance of the CO line by setting the DC voltage on the input cavity mirror PZT. The carrier thus strongly interacts with the gas, unlike its sidebands, too far from resonance, which become local oscillators used for the heterodyne detection. We band-pass filter the  $f_{FSR}$  component of the signal from the transmission photodiode and mix it with the 585 MHz source. The obtained error signal is optimized by setting the detection phase to dispersion using the phase delay  $\Delta\Phi_1$  between the two RF signals.

To improve the S/N and baseline stability, we dither the cavity length (on the PZT of the output mirror) at the frequency  $f_{dith} = 149$  Hz which happens to be a local minimum in the observed power spectral density of the RF balanced mixer. The frequency deviation of the applied dither is about 100 kHz. The demodulated low-pass filtered error signal is the input to a lock-in amplifier (SRS model SR830) for derivative locking [19] and the  $2f$  signal is fed back to the cavity input mirror PZT.

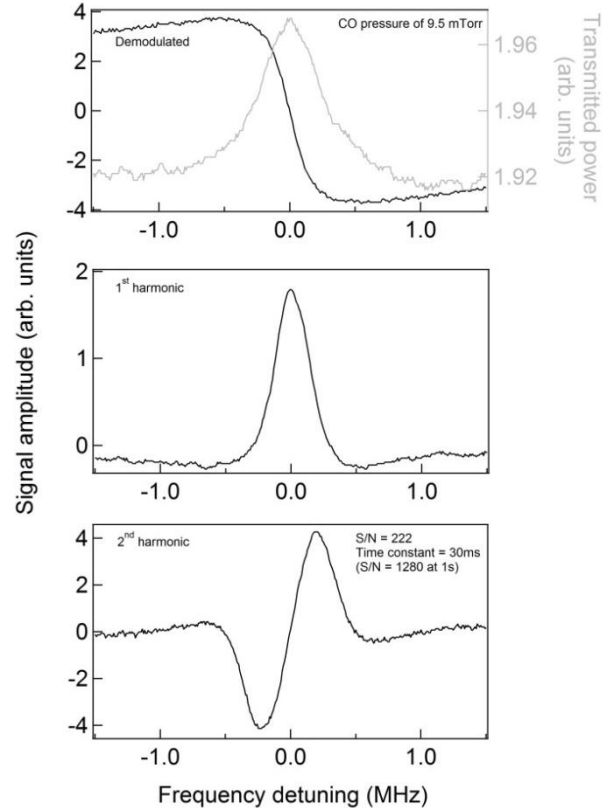


Fig. 2. Top: Sub-Doppler transmission peak (in grey) and demodulated NICE-OHMS signal (in black). Center and Bottom: Dither lock-in detection of the NICE-OHMS signal at the first and second harmonics.

On the top plot in Figure 2, the transmitted sub-Doppler peak is shown in grey along with the demodulated NICE-OHMS signal

as a function of the frequency detuning from line center. The linewidth of the saturated absorption peak is measured at about 400 kHz, mainly due to the transit time broadening and pressure broadening as calculated above. The demodulated signal shows a S/N of 183, measured in a 1 Hz bandwidth yielding a S/N of 458 at 1 second. The center and bottom plots show the demodulated signals at the  $1f$  and  $2f$  harmonics of the dithered NICE-OHMS signal at the output of the lock-in amplifier. The time constant of the lock-in amplifier was set at 30 ms and the measured S/N for the  $1f$  and  $2f$  harmonics was 216 and 222, respectively. Therefore, the S/N at 1 second is calculated at 1249 and 1280 respectively. The fractional stability of our frequency standard is the transit-time, pressure and power broadened molecular linewidth divided by the S/N of the  $2f$  signal at 1 second. Therefore, based on the measured S/N, the fractional frequency stability works out to  $1.63 \times 10^{-12}$  at 1 second. Additionally, the detection sensitivity based on the absolute level of saturated absorption calculated earlier and the S/N of the  $1f$  detected signal works out to  $5.5 \times 10^{-10}$  at 1 second.

We evaluated the frequency stability of our NICE-OHMS based molecular clock system by comparing it to a frequency comb. Once all servos are engaged at optimal working points, we pick off one part of the incident beam right after the fiber-coupled AOM, and generate a beat signal with the stabilized frequency comb (Menlo Systems, FC1550). The 250 MHz repetition rate of the comb is stabilized by locking one tooth to a temperature-stabilized auxiliary high-finesse Fabry-Perot cavity ( $Finesse = 130,000$ ) in vacuum with a measured drift  $<1$  Hz per second. The cavity fractional frequency instability is below  $10^{-14}$  at 1 second. The beatnote RF frequency is logged with a frequency counter (Keysight, 53230A). The offset frequency of the frequency comb is 10 MHz and it is stabilized to a hydrogen maser (T4Science, iMaser3000) that has a measured fractional frequency instability of  $10^{-13}/\sqrt{\tau}$ , where  $\tau$  is the averaging time. Figure 3 shows the obtained fractional frequency stability of the NICE-OHMS based CO frequency standard wherein the Allan deviation is  $1.8 \times 10^{-12}$  at 1 second, and averages down as  $1/\sqrt{\tau}$  to  $3 \times 10^{-14}$  at 1000 seconds.

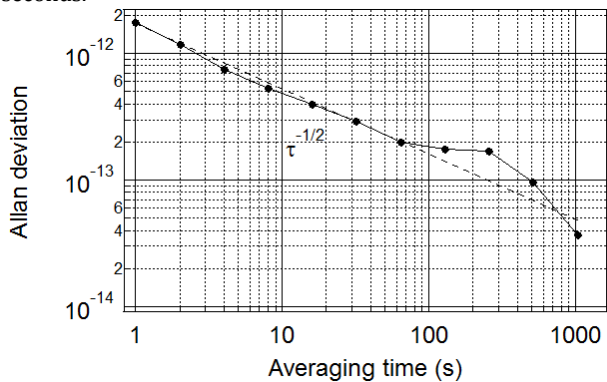


Fig. 3. Allan deviation versus averaging time of the beat-note between the NICE-OHMS frequency stabilized system and a cavity-stabilized frequency comb.

The bump in the plot appears to be caused by the air conditioning cycle in the laboratory. The value at 1 second is consistent with the number calculated above by considering the measured S/N from Fig. 2. The Fabry-Perot cavity shows lower frequency instability at short times, mainly limited by the noise of the PZTs holding the cavity mirrors.

It is clear that our detection system has good sensitivity, but has not reached the shot-noise floor. S/N limitations arise from

technical noise, frequency jitter, scattered light, residual amplitude modulation (RAM) and radiated coupling from the relatively high 585 MHz FSR frequency. However, we are working to improve the S/N of our detection system by using isolators and resonant photodetectors in transmission, optimization and shielding of the electronic layout. In order to reduce piezo noise, we plan to use shorter piezos and also attempt to place piezo rings around the ULE cavity for length control. We are customizing the laser source to interrogate the stronger R(7) absorption line at 1568.038nm that should roughly double the molecular contrast. We are reducing the transit-time line broadening through an increase in the cavity mode size by the use of high ROC mirrors ( $>5$  m). We are in the process of building a second CO spectrometer for direct frequency stability measurements and optimization of the spectroscopic, optical and electronic parameters in a systematic manner to approach the shot-noise limit of the frequency standard.

In summary, we have demonstrated the first laser frequency stabilization scheme with a molecular  $^{12}\text{C}^{16}\text{O}$  overtone transition, using the NICE-OHMS method. The measured frequency instability is  $1.8 \times 10^{-12}$  at 1 second and  $3.5 \times 10^{-14}$  at 1000 seconds.

**Funding.** NASA Strategic Astrophysics Technology (SAT) program “Physics of the Cosmos” (PCOS) under grant #NNX13AC91G.

**Acknowledgements.** The authors would like to thank J.L. Hall for useful discussions and use of his modeling spreadsheet. We would also like to thank Leo Hollberg at Stanford University for providing access to the frequency comb for clock stability measurements, K. Urbanek and S. Tan for help with the optics.

## References

1. K. Danzman et.al., *Class. And Quantum Gravity*, **13**, A247 (1996).
2. J. Lipa, S. Buchman, S. Saraf, J. Zhou, A. Alfauwaz, J. Conklin, G.D. Cutler, and R.L. Byer, *arXiv:1203.3914v1[gr-qc]* (2012).
3. T. Schuldt, S. Saraf, A. Stochino, K. Doringshoff, S. Buchman, G. D. Cutler, J. Lipa, S. Tan, J. Hanson, B. Jaroux, C. Braxmaier, N. Gurlebeck, S. Herrmann, C.Lammerzahl, A. Peters, A. Alfauwaz, A. Alhussien, B. Alsuwaidan, T. Al Saud, H. Dittus, U. Johann, S.P. Worden, and R.L. Byer, *IFCS-EFTF* (2015).
4. E. J. Zang, J. P. Cio, C. Y. Li, Y. K. Deng, and C. Q. Gao, *IEEE Trans. on Inst. And Meas.* **56**, 673 (2007).
5. J. Ye, L. Ma, and J. L. Hall, *Opt. Lett.* **21**, 1000 (1996).
6. L. Ma, J. Ye, P. Due, and J. L. Hall, *J. Opt. Soc. Am. B*, **16**, 2255 (1999).
7. J. Ye, L. S. Ma, and J. L. Hall, *J. Opt. Soc. Am. B*, **15**, 6 (1998).
8. J. L. Hall, private communication.
9. A. Foltynowicz, F. M. Schmidt, W. Ma, and O. Axner, *Appl. Phys. B* **92**, 313 (2008).
10. N. Leeuwen and A. C. Wilson, *J. Opt. Soc. Am. B* **21**, 1713 (2004).
11. W.C. Swann and S.L. Gilbert, *J. Opt. Soc. Am. B*, **19**, 2461 (2002).
12. J. Henningsen, H. Simonsen, T. Møgelberg, and E. Trudso, *Journal of Mol. Spect.* **193**, 354 (1999).
13. L. S. Rothman, I. E. Gordon, Y. Babikov, A. Barbe, D. Chris Benner, P. F. Bernath, *JQSRT* **130**, 4 (2013).
14. P. H. Krupenie, *NSRDS-NBS 5* (1966).
15. K. Numata, J. Camp, M. A. Krainak, and L. Stolpner, *Opt. Express* **18**, 22781 (2010).
16. R. Drever, J. L. Hall, F. V. Kowalski, J. Hough, G. M. Ford, A. J. Munley, and H. Ward, *Appl Phys B* **31**, 97 (1983).
17. G. Domenico, S. Schilt, and P. Thomann, *Appl. Opt.* **49**, 4801 (2010).
18. R.G. DeVoe and R.G. Brewer, *Phys. Rev. A* **30**, 5, 2827 (1984).
19. H. Wahlquist, *J. Chem. Phys.* **35**, 1708 (1961).

## FULL REFERENCES

1. K. Danzman and the LISA study team, "LISA: laser interferometer space antenna for gravitational wave measurements," *Classical and Quantum Gravity*, **13**, A247 (1996).
2. J. Lipa, S. Buchman, S. Saraf, J. Zhou, A. Alfauwaz, J. Conklin, G.D. Cutler, and R.L. Byer, "Prospects for an advanced Kennedy-Thorndike experiment in low Earth orbit," *arXiv:1203.3914v1 [gr-qc]* (2012).
3. T. Schuldt, S. Saraf, A. Stochino, K. Doringshoff, S. Buchman, G. D. Cutler, J. Lipa, S. Tan, J. Hanson, B. Jaroux, C. Braxmaier, N. Gurlebeck, S. Herrmann, C. Lammerzahn, A. Peters, A. Alfauwaz, A. Alhussien, B. Alsuwaidan, T. Al Saud, H. Dittus, U. Johann, S.P. Worden, and R.L. Byer, "mSTAR: Testing Special Relativity in Space Using High Performance Optical Frequency References," *IEEE International Frequency Control Symposium & European Frequency and Time Forum Proceedings*, Denver, Colorado, April 2015
4. E. J. Zang, J. P. Cao, Y. Li, C. Y. Li, Y. K. Deng, and C. Q. Gao, "Realization of four-pass I2 absorption cell in 532-nm optical frequency standard," *IEEE Trans. Instrum. Meas.* **56**, 673-676 (2007).
5. J. Ye, L. S. Ma, and J. L. Hall, "Sub-Doppler optical frequency reference at 1.064  $\mu\text{m}$  by means of ultrasensitive cavity-enhanced frequency modulation spectroscopy of a C<sub>2</sub>H<sub>2</sub> overtone transition," *Opt. Lett.* **21**, 1000-1002 (1996).
6. L. S. Ma, J. Ye, P. Dube, and J. L. Hall, "Ultrasensitive frequency-modulation spectroscopy enhanced by a high finesse optical cavity: theory and application to overtone transitions of C<sub>2</sub>H<sub>2</sub> and C<sub>2</sub>H<sub>2</sub>D," *J. Opt. Soc. Am. B* **16**, 2255-2268 (1999).
7. J. Ye, L. S. Ma, and J. L. Hall, "Ultrasensitive detections in atomic and molecular physics: demonstration in molecular overtone spectroscopy," *J. Opt. Soc. Am. B* **15**, 6-15 (1998).
8. J. L. Hall, private communication.
9. A. Foltynowicz, F. M. Schmidt, W. Ma, and O. Axner, "Noise-immune cavity-enhanced optical heterodyne molecular spectroscopy: current status and future potential," *Appl. Phys. B* **92**, 313-326 (2008).
10. N. J. Van Leeuwen and A. C. Wilson, "Measurement of pressure-broadened, ultraweak transitions with noise-immune cavity-enhanced optical heterodyne molecular spectroscopy," *J. Opt. Soc. Am. B* **21**, 1713-1721 (2004).
11. W. C. Swann, S. L. Gilbert, "Pressure-induced shift and broadening of 1560-1630-nm carbon monoxide wavelength-calibration lines," *J. Opt. Soc. Am. B* **19**, 2461-2467 (2002).
12. J. Henningsen, H. Simonsen, T. Møgelberg, and E. Trudso, "The  $0 \rightarrow 3$  Overtone Band of CO: Precise Linestrengths and Broadening Parameters," *Journal of Molecular Spectroscopy* **193**, 354-362 (1999).
13. L. S. Rothman, I. E. Gordon, Y. Babikov, A. Barbe, D. Chris Benner, P. F. Bernath, "The HITRAN2012 molecular spectroscopic database," *JQSRT* **130**, 4-50 (2013).
14. P. H. Krupenie, "The Band Spectrum of Carbon Monoxide," NSRDS-NBS 5, National Standard Reference Data Series, NBS- 5 (1966).
15. Kenji Numata, Jordan Camp, Michael A. Krainak, and Lew Stolpner, "Performance of planar-waveguide external cavity laser for precision measurements," *Opt. Express* **18**, 22781-22788 (2010)
16. R. W. P. Drever, J. L. Hall, F. V. Kowalski, J. Hough, G. M. Ford, A. J. Munley, and H. Ward, "Laser phase and frequency stabilization using an optical resonator," *Appl. Phys. B* **31**, 97-105 (1983).
17. Gianni Di Domenico, Stéphane Schilt, and Pierre Thomann, "Simple approach to the relation between laser frequency noise and laser line shape," *Appl. Opt.* **49**, 4801-4807 (2010)
18. R. G. DeVoe and R. G. Brewer, "Laser frequency division and stabilization," *Phys. Rev. A* **30**, 2827-2829 (1984).
19. H. Wahlquist, "Modulation Broadening of Unsaturated Lorentzian Lines," *J. Chem. Phys.* **35**, 5, 1708-1710 (1961).